Molecular Structure and Spectroscopy of a Bacteriopurpurin. A New Class of Bacteriochlorin Photosensitizers

Byron C. Robinson,*,[1a] Kathleen M. Barkigia,[1b] Mark W. Renner,[1b] and Jack Fajer*,[1b]

Miravant Medical Technologies, Santa Barbara, California 93117, and Department of Applied Science, Brookhaven National Laboratory, Upton, New York 11973

Received: April 2, 1999; In Final Form: June 22, 1999

Bacteriochlorins mediate energy and electron transfer in vivo and serve as biomimetic models of bacterial photosynthesis. Recently, the same physicochemical properties of the chromophores have made them attractive as photosensitizers for photodynamic therapy, a medical treatment that combines light, porphyrins, and oxygen to attack and destroy malignant tissue. Despite this intense biophysical, chemical, and medicinal interest in bacteriochlorins, very few high precision structures of the chromophores exist to provide the basis for theoretical calculations that seek to predict their extensively studied physicochemical properties. We report here the synthesis, spectral characterization, and structural determination of a metal-free bacteriopurpurin **1**, a paradigm for a new class of photosensitizers comprised of porphyrins at the saturation level of bacteriochlorins flanked by two annelated, exocyclic cyclopentenyl rings. The molecule exhibits a very red-shifted Qy transition at 843 nm and is readily oxidized (at 0.39V vs SCE) to a π cation radical with a distinctive EPR signal. The crystallographic results for **1** unambiguously identify the bacteriopurpurin, provide the first stereochemical parameters for this new class of expanded bacteriochlorins, extend the high resolution structural database for bacteriochlorins, and form the basis for theoretical calculations which correctly describe the optical features and electron density profile of **1** and its cation radical.

Introduction

Recent crystallographic studies of antenna and reaction center bacteriochlorophyll (BChl) proteins[2,3] are unveiling the architecture used by photosynthetic bacteria to harvest and transduce light into chemical energy. However, the overriding major benefit of protein crystallography, i.e., determination of the structure of macromolecules with molecular weights of tens of thousands, is limited by the resolution inherent to such large arrays, which results in precisions on the order of 0.1−0.5 Å in the BChl structures reported to date.[2,3] In contrast, structures of isolated chromophores can be determined to precisions of 0.005 Å and offer experimentalists and theoreticians supplemental insights into stereochemical features less readily available from protein determinations.[4] Surprisingly, despite the intense experimental and theoretical focus on chromophores that mediate or model natural and artificial photosynthesis, there exists a dearth of high precision structural data for bacteriochlorins[4,5] that would serve to validate and calibrate theoretical treatments of their optical, redox, EPR, NMR, electron and energy transfer properties.[6]

In a different but not unrelated context, the crucial role of BChls in photochemical energy and electron transfer as well as the shifts of the Qy transitions of the chromophores to the near infrared region have recently focused attention on bacteriochlorins as potential sensitizers for photodynamic therapy (PDT).[7−9] This medical treatment employs a combination of light, drugs (porphyrins in this case) and oxygen to induce necrotic effects on targeted cancerous tissues. Advantages of bacteriochlorins include the bathochromism of the Qy bands which allows deeper tissue penetration of the exciting light and the fact that photoexcited bacteriochlorins can potentially function as generators of singlet oxygen (type II photoprocess) as well as induce electron transfer (type I) because they are easily oxidized. Two bacteriochlorins recently investigated for PDT consist of a BChl *a*-serine complex[8] and a BChl *a* derivative, bacteriochlorin *a*,[9] which absorb light in the 760−780 nm region.

PDT is obviously not limited to bacteriochlorins and seeks to take advantage of the vast and expanding panoply of porphyrin derivatives as "second-generation" photosensitizers. A considerable effort is now also devoted to purpurins,[7,10−13] porphyrins with annelated cyclopentenyl rings which are formally at the same saturation level as chlorins, and typically absorb light in the 650−715 nm region. One of these, dichloro tin (IV) etiopurpurin ethyl ester is in phase III clinical trials.[1a] Structures of purpurins are even scarcer than those of bacteriochlorins. To date, only a single crystallographic determination of a purpurin has been reported, that of 5,15-di (4-pyridyl)-octaethylpurpurin (purp 515).[13]

We report here the synthesis, spectroscopy and structural characterization of a bacteriopurpurin, a new class of purpurins with two annelated cyclopentenyl exocyclic rings (see Figure 1). The new compound **1** exhibits a strong Qy band at 843 nm, the most bathochromic shift for any monomeric bacteriochlorin, and the compound is easily oxidized to a π cation radical. The crystallographic determination extends the high precision structural database for bacteriochlorins and purpurins, and provides the first unambiguous identification and stereochemical parameters for this new class of expanded purpurins. In addition, it offers the opportunity to treat these compounds theoretically, an avenue of research heretofore not possible because of a lack of (any) high precision crystallographic data. Calculations based on the crystal coordinates reported here do correctly describe

* To whom Correspondence should be addressed. Department of Applied Science, Brookhaven National Laboratory, Upton, NY 11973. Tel.: (516) 344−4521. Fax: (516) 344−3137. E-mail: fajerj@bnl.gov.

10.1021/jp991138a CCC: $18.00
Published on Web 08/10/1999

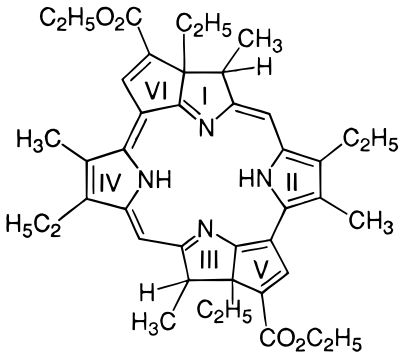

Figure 1. Structural formula of the bacteriopurpurin **1**.

the optical features, orbital occupancy, and electron density profile of **1** and its radical, and thus proffer the promise of guiding the design and predicting the physicochemical properties of new photosensitizers.

Methods

The bacteriopurpurin **1** was synthesized as follows: 5,15-bis-acrylate etioporphyrin I[14] (100 mg) was dissolved in toluene (20 mL) and 1,8-diazobicyclo[5.4.0] undec-7-ene was added. The solution was refluxed under argon for 5 h after which the solvent was removed by rotary evaporation. The residue was dissolved in CH_2Cl_2 (10 mL) and was run through a silica gel 60 column (230−400 mesh, Merck) using CH_2Cl_2 as the eluent. The major green fraction was collected and evaporated to dryness. The solid was dissolved in CH_2Cl_2 (5 mL) and methanol (10 mL) was added. CH_2Cl_2 was removed by slow rotary evaporation and the precipitated solid **1** collected by filtration. The solid was pumped dry under vacuum to yield 175 mg (88%) of **1**. ^{1}H NMR spectra were recorded on a Varian 500 MHz spectrometer in $CDCl_3$. Chemical shifts are expressed in ppm relative to the $HCCl_3$ signal set at 7.24 ppm vs TMS. Shifts are assigned to specific atoms according to the numbering system in Figure 2, i.e., 22-CH_3 is the methyl group comprised of atom 22. ^{1}H NMR (δ, ppm): −0.08 (t, 6H, 22-C**H**$_3$ and 33-C**H**$_3$), 0.61 (s, 2H, 2 × N**H**), 1.54 (t, 6H, 31-C**H**$_3$ and 42-CH_3), 1.57 (t, 6H, 25-C**H**$_3$ and 36-C**H**$_3$), 1.65 (m, 2H, 21-C**H**$_a$ and 32-C**H**$_a$), 2.35 (d, 6H, 23-C**H**$_3$ and 34-C**H**$_3$), 2.57 (m, 2H, 21-C**H**$_b$ and 32-C**H**$_b$), 3.33 (s, 6H, 26-C**H**$_3$ and 37-C**H**$_3$), 3.58 (m, 4H, 24-C**H**$_2$ and 35-C**H**$_2$), 4.20 (q, 2H, 3-C**H** and 13-C**H**), 4.49 (q, 4H, 30-C**H**$_2$ and 41-C**H**$_2$), 8.19 (s, 2H, 5,15-meso-**H**), 9.29 (s, 2H, 27-C**H** and 38-C**H**).

High-resolution mass spectra were obtained from the mass spectrometry unit of the University of California at Santa Barbara. MS calcd for **1**: 674.3832. Found: 674.3817. Optical spectra were recorded on a Cary 500 spectrophotometer in CH_2Cl_2 λ_{max}, nm (ϵ, M^{-1} cm^{-1}): 364 (32100), 416 (60600), 439 (40600), 559 (15800), 593 (79300), 768 (8300), 791 (9330), 843 (70800). (See also Figure 7, below). Redox potentials were determined by cyclic voltammetry in CH_2Cl_2 with 0.1M Bu_4NClO_4 as supporting electrolyte on a BAS 100A electrochemical analyzer. Solvents were dried and distilled immediately before use. The π cation radical of **1** was generated by reaction with $AgClO_4$. Electron paramagnetic resonance (EPR) spectra of the radical were recorded on a Bruker ESP 300E spectrometer. Optical spectra were calculated with the INDO/s (intermediate neglect of differential overlap) method developed by Zerner and co-workers for optical spectra of porphyrins.[15] The method consists of a ground-state self-consistent field calculation followed by monoexcited configuration interaction. Excitations were generated from an active space comprised of 11 HOMOs and 11 LUMOs. The coordinates reported here were used for the INDO/s calculations as well as for iterative extended Hückel (IEH) calculations[16] of the unpaired spin density profile of the cation radical.

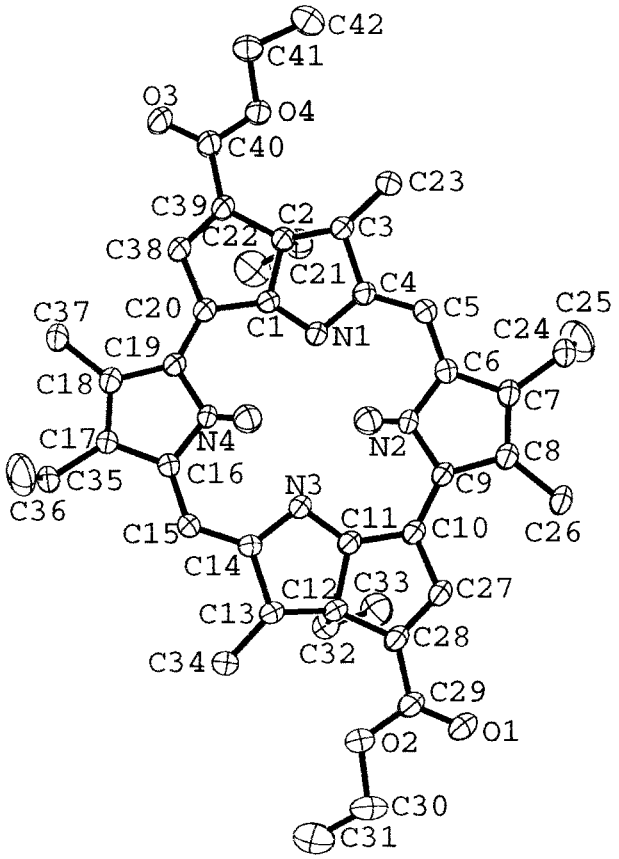

Figure 2. Molecular structure and atom names for **1**. Thermal ellipsoids of the carbon, oxygen and nitrogen atoms enclose 50% probabilities. Peripheral hydrogens are omitted for clarity.

The bacteriopurpurin $C_{42}H_{50}O_4N_4 \cdot 0.25(C_6H_{14})$ crystallized from a mixture of alkanes/THF in space group $C2/c$ with a = 22.241 (2) Å, b = 16.730(2) Å, c = 23.858(2) Å, β = 111.34(1)°, V = 8268.7(15) Å^3, and Z = 8. Because of the small crystal size, 0.063 × 0.073 × 0.088 mm, data were collected at beamline X7B of the Brookhaven National Synchrotron Light Source at 200K with λ = 0.8798 Å using a MAR 345 imaging plate detector. A total of 51732 reflections ($\pm h$ $\pm k$ $\pm l$) were recorded and processed with DENZO/SCALEPACK to give 6752 unique reflections. The structure was solved with SHELXS-86 and refined with SHELXL-93 to R1 = 0.085, wR2 = 0.256 for the 5935 data with $I > 2\sigma(I)$, and R1 = 0.097 and wR2 = 0.281 for 6740 data. Additional details of the refinement and complete sets of coordinates, bond distances, and angles are included in the Supporting Information.

Results

1. Crystallography. The molecular structure of **1** and atom names are shown in Figure 2. The crystallographic data of Figure 3 establish that the molecule is indeed a bacteriopurpurin comprised of two opposite pyrrole rings (II and IV) and two oppositely saturated pyrroline rings (I and III) flanked by exocyclic rings (V and VI). The bond distances in Figure 3 present a highly symmetrical pattern with near $\bar{1}$ symmetry and good internal consistency among equivalent bonds. The bond distances within the pyrrole rings II and IV are typical of those found in porphyrins and contrast with the longer bonds in rings I and III which establish that those are saturated rings with average Cβ−Cβ (C2−C3 and C12−C13) bond lengths of 1.570-

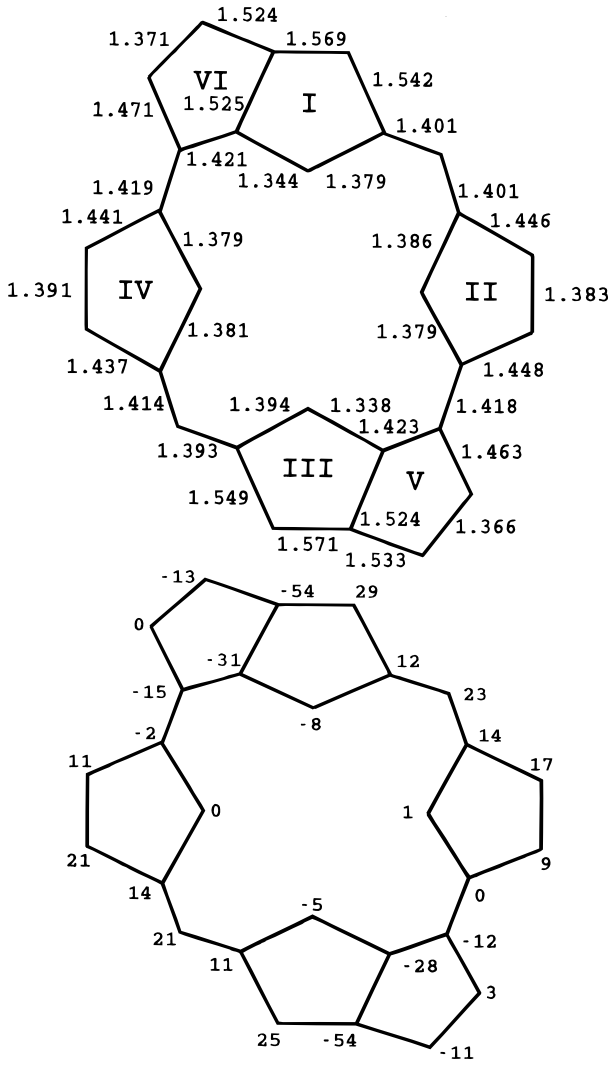

Figure 3. (Top) Bond distances for **1**, in angstroms. The average esd for a typical C−C bond is 0.004 Å. (Bottom) Displacements of the 28 atoms that comprise the bacteriopurpurin core of **1** from the 24 atom "porphyrin" mean plane (C1−C20 including N1−N4), in units of 0.01 Å.

(4) Å and average Cα−Cβ (C1−C2, C3−C4, C11−C12, C13−C14) bonds of 1.535(4) Å typical of single bonds.[4] Unusual features of rings I and III are the shortened N1−C1 and N3−C11 bonds of 1.344(4) Å and 1.338(4) Å which are adjacent to the five-membered exocyclic rings. These short C_α−N bonds appear to be typical of purpurin derivatives, the analogous bond in purp 515 is 1.331(4) Å.[13] As well, the Cα−N−Cα angles in rings I and III are significantly more compressed, 106.2(3)°, than the corresponding angles normally found in the saturated rings of bacteriochlorin derivatives,[4] 108−109°. Note also that C20−C38 and the equivalent C10−C27 bonds in the exocyclic rings are shorter than expected for pure single bonds, 1.471(4) Å and 1.463(4) Å, suggesting conjugation of the exocyclic double bonds C38−C39 and C27−C28 with the porphyrin π system.

A marked difference between the bacteriopurpurin and hydroporphyrins occurs in the Ct−N distances. In hydroporphyrins, the Ct−N distances to the saturated rings are longer than those to the pyrrole rings.[4,5] In contrast, in **1**, the distances to rings I and III average 1.939(4) Å and those to rings II and IV average 2.201(4) Å. In purp 515, the Ct−N distance to the saturated ring is also the shortest, 1.963 Å.

The skeleton of **1** is slightly ruffled. Displacements from the mean "porphyrin" plane comprised of atoms C1 through C20 and N1 through N4 are given in Figure 3. (The same pattern is found when the displacements are calculated relative to the plane of the four nitrogens.) Rings II and IV lie slightly above that plane, whereas rings I and III are twisted above and below the plane. The largest deviations of −0.54 Å occur at the tetrahedral carbons C2 and C12. The nonplanarity of the saturated rings is further illustrated in the edge-on-view of ring I shown in Figure 4 (Ring III is essentially the same). The torsion angles about the Cβ-Cβ bonds reflect the distortions of rings I and III: they are 28.9° around C2−C3 and 28.6° around C12−C13. In contrast, the comparable torsion angles in rings II and IV are 0.5° and −0.1° about C7−C8 and C17−C18, respectively. For comparison, the torsion angle in the single saturated ring of purp 515 is 30.8°. Figure 4 also illustrates the syn configuration of the alkyl substituents at C2 and C3, i.e., the alkyl groups orient on the same side of the porphyrin face (the same configuration is also found at C12 and C13.) Although the present structural results do not establish the absolute stereochemistry at C2, C3, C12, and C13, the relative orientations of the substituents at these positions are unambiguously syn and confirm the same configuration noted in the purp 515 structure. The molecules of **1** pack in pairs with rings I and II partially overlapping rings II and I of an inversion-related molecule, as illustrated in Figure 5. The mean plane separation of 3.61 Å, Ct−Ct distance of 5.06 Å, lateral shift of 3.55 Å, and slip angle of 44.6° are all indicative of π−π interactions.

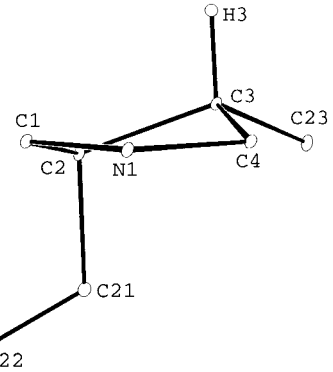

Figure 4. Edge-on-view of ring I which illustrates the syn orientation of the alkyl substituents at C2 and C3. The same orientation is found for the equivalent substituents at C12 and C13.

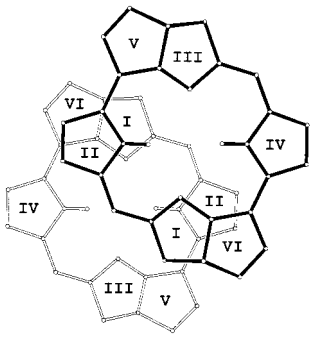

Figure 5. Illustration of the stacking of inversion-related molecules. The mean plane separation is 3.61 Å.

Despite the intense interest in the use of porphyrin derivatives for photodynamic therapy, there exist few stereochemical data that might provide insights into the mechanisms by which the photosensitizers localize or sequester in malignant tissues. To illustrate the size and volume of the bacteriopurpurin, Figure 6 presents a space-filling model of **1** generated by drawing van der Waals radii around every atom of the molecule, including the hydrogens.

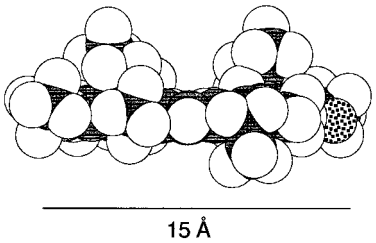

Figure 6. Space-filling version of Figure 2 generated by drawing van der Waals radii around each atom including the hydrogens.

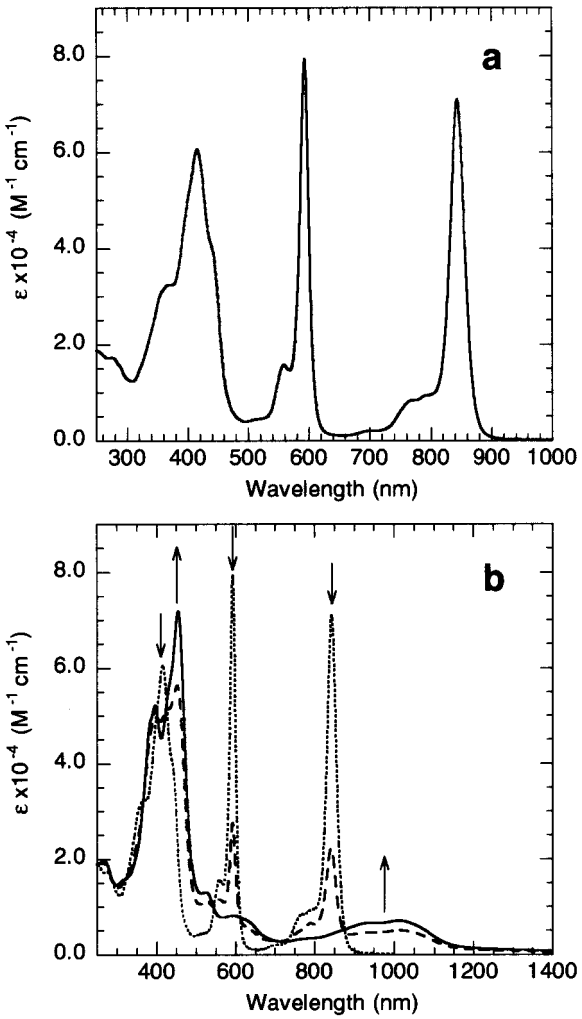

Figure 7. a) Optical spectrum of **1** in CH_2Cl_2. b) Optical spectra of **1** (···) and of its π cation radical, $\mathbf{1}^{+\bullet}$ ClO_4^- (—) in CH_2Cl_2. An intermediate stage in the oxidation is also shown (– –) to illustrate the isosbestic points observed as the reaction progresses.

2. Spectroscopy and Calculations. The optical spectrum of **1** in CH_2Cl_2 is shown in Figure 7a. A nearly identical spectrum is observed in methanol and thus minimizes the possibility that the spectrum observed is due to the $\pi-\pi$ aggregation seen in the crystal structure. The salient feature of the spectrum is the bathochromic shift of the Qy transition to 843 nm compared to those of other bacteriochlorins or bacteriochlorophylls. To our knowledge, the band at 843 nm represents the most red-shifted Qy transition of any existing natural or synthetic monomeric bacteriochlorin derivative.[5,7−9,17−20]

An INDO calculation based on the coordinates of **1** reported here predicts a HOMO to LUMO transition at 839 nm (11919 cm^{-1}) in good agreement with the experimental value of 843 nm (11862 cm^{-1}) in CH_2Cl_2.

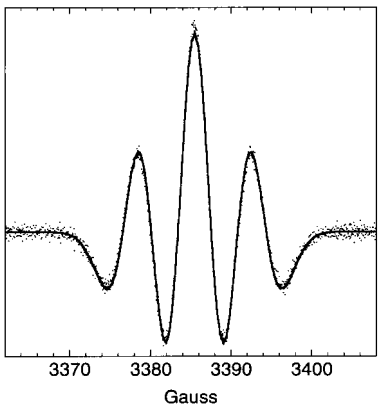

Figure 8. Second derivative EPR spectrum of $\mathbf{1}^{+\bullet}$ ClO_4^- in CH_2Cl_2 over which is superimposed a simulation (—) which demonstrates that 2 equivalent protons determine the major features of the spectrum (a_H = 6.45G, T = 270K).

Cyclic voltammetry provides a direct measure of the ease of oxidation (E_{ox}) and reduction (E_{red}) for the new molecule. Furthermore, the difference between the first oxidation and reduction potentials provides a complementary experimental probe of the energy gap between the HOMO and LUMO (neglecting solvation effects) such that $E_{ox} - E_{red} \approx E$ optical.[21] In CH_2Cl_2, **1** undergoes reversible one-electron oxidation and reduction steps at 0.39V and −1.00V, respectively, versus SCE. The difference between the two, 1.39V, compares reasonably well with the energy of 1.47 eV for the HOMO to LUMO optical transition of **1**. It is also instructive to compare the redox potentials and Qy transition of **1** with those of other bacteriochlorins. For free base 5,10,15,20-tetraphenylbacteriochlorin[17] (H_2TPBC), E_{ox} = 0.40V, E_{red} = −1.10V, with the Qy transition at 740 nm. For bacteriopheophytin *a*,[18] E_{ox} = 0.82V, E_{red} = −0.84V, λ_{mas} = 745 nm, and for bacteriochlorophyll *a*,[18,22,23] E_{ox} = 0.40V, E_{red} = −1.10V, λ_{max} = 774 nm.

Because of its low oxidation potential, **1** is readily oxidized with I_2 or $AgClO_4$ in CH_2Cl_2. The optical spectra of the oxidized product and of an intermediate stage in the oxidation are shown in Figure 7. The spectrum is characterized by new bands in the near-infrared region around 1000 nm, loss of the strong 843 and 559 nm bands, and a red-shift of the Soret bands. These optical changes parallel those observed upon oxidation of bacteriochlorins and bacteriochlorophylls and are diagnostic of bacteriochlorin π cation radicals.[17,24]

The radical nature of the oxidation product is unambiguously established by its EPR spectrum which is shown in Figure 8. A simulation which assumes that two equivalent protons with hyperfine coupling constants (hfcs) of 6.45G determine the major features of the spectrum yields a near perfect fit to the experimental data, see Figure 8. (The broad line width used in the simulation obviously subsumes smaller hfcs from other nucleii). The unpaired spin density profile of $\mathbf{1}^+$ in Figure 9, obtained by an iterative extended Hückel calculation, reveals that electron density is principally localized on the α carbons of the molecule, i.e., an "a_{1u}" profile similar to those of other chlorins and bacteriochlorins[17,24] (the a_{1u} nomenclature, originally developed for porphyrins with D4h symmetry, is traditionally retained for hydroporphyrins.) Given the a_{1u} spin profile calculated for the radical, examination of Figures 9 and 1 shows that only the single protons on the β carbons of rings I and III would sample and report the high spin densities predicted for the α-carbons. The large hfcs of 6.45G observed experimentally are thus assigned to the single protons at C3 and C13 of rings I and III, respectively. In general accord with this conclusion,

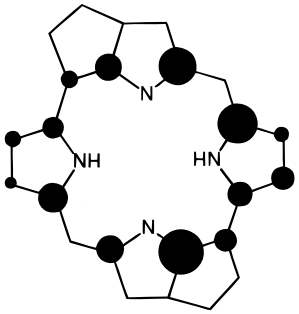

Figure 9. Calculated unpaired spin density profile for the π cation radical $\mathbf{1}^{+\bullet}$. The diameters of the circles are proportional to the spin densities.

an INDO/RHF/SP calculation,[25] also based on the present coordinates, predicts hfcs of 8.6 G for those two protons[26] (Recall that these are β protons whose observed hfcs obey a $\rho\cos^2\theta$ relationship and depend on the unpaired spin density ρ at the α carbons C4 and C14 as well as on the dihedral angle θ between the p_z orbitals at those carbons and the reporting protons.[24] The calculated hfcs for those sites will therefore be acutely sensitive to the spatial orientations of the protons relative to the p_z orbitals at the α carbons. (See Figure 4 for an example: the proton H3 samples the spin density at the α carbon C4)

The large hfcs of the protons on the saturated rings I and III also parallel those observed in other bacteriochlorin π cation radicals. In $H_2TPBC^{+\bullet}$ and $ZnTPBC^{+\bullet}$, these fall between 7.5 and 8.1G,[17,24] whereas in BChl $a^{+\bullet}$ and BPheo $a^{+\bullet}$ they range between 4.1 and 6.7G.[24,27]

In conclusion, we have described here the synthesis, spectroscopy and structural characterization of a bacteriopurpurin, a new class of expanded bacteriochlorins. The new compound retains many of the electronic properties of bacteriochlorins. In addition, it exhibits the most bathochromically shifted Qy transition of any natural or synthetic monomeric bacteriochlorin, and it is also easily oxidized to a π cation radical. Both features make it attractive as a potential photosensitizer for PDT and, obviously, for artificial photosynthesis as well. The crystallographic determination provides the first unambiguous identification and stereochemical parameters for this new class of expanded purpurins. In addition, it affords the opportunity to treat the compound theoretically, an avenue of research previously not possible because of a lack of high precision crystallographic data. Calculations based on the crystal coordinates reported here do correctly describe the optical features, orbital occupancy and electron density profile of **1** and its radical, and thus offer the promise of guiding the design and predicting the physicochemical properties of new photosensitizers of this type.

Acknowledgment. We thank Dr. Martin Plato and Matthias Wittenberg (Free University of Berlin) for the INDO/RHF/SP results for $\mathbf{1}^{+\bullet}$ and Dr. Jonathan C. Hanson for assistance with the crystallographic data collection. The work at Brookhaven was supported by the Division of Chemical Sciences, U.S. Department of Energy, under Contract DE-AC02-98CH10886.

Supporting Information Available: For **1**: experimental crystallographic details, atomic coordinates, bond distances and angles, anisotropic thermal parameters, and hydrogen coordinates. This material is available free of charge via the Internet at http://pubs.acs.org.

References and Notes

(1) (a) Miravant Medical Technologies. (b) Brookhaven National Laboratory

(2) Freer, A.; Prince, S.; Sauer, K.; Papiz, M.; Hawthornthwaite-Lawless, A.; McDermott, G.; Cogdell, R.; Isaacs, N. W. *Structure* **1996**, *4*, 449. Koepke, J.; Hu, X.; Muenke, C.; Schulten, K.; Michel, H. *Structure* **1996**, *4*, 581. Li, Y. F.; Zhou, W.; Blankenship, R. E.; Allen, J. P. *J. Mol. Biol.* **1997**, *271*, 456.

(3) Ermler, U.; Fritzsch, G.; Buchanan, S. K.; Michel, H. *Structure* **1994**, *2*, 925. Deisenhofer, J.; Epp, O.; Sinning, I.; Michel, H. *J. Mol. Biol.* **1995**, *246*, 429.

(4) Barkigia, K. M.; Fajer, J. *The Photosynthetic Reaction Center*; Deisenhofer, J., Norris, J. R., Eds.; Academic Press: San Diego, CA, 1993; Vol. II, p 513.

(5) For examples of bacteriochlorin structures, see: Barkigia, K. M.; Fajer, J.; Chang, C. K.; Young, R. *J. Am. Chem. Soc.* **1984**, *106*, 6457. Waditschatka, R.; Kratky, C.; Jaun, B.; Heinzer, J.; Eschenmoser, A. *J. Chem. Soc., Chem. Commun.* **1985**, 1604. Barkigia, K. M.; Miura, M.; Thompson, M. A.; Fajer, J. *Inorg. Chem* **1991**, *30*, 2233. Senge, M. O.; Runge, S. *Acta Crystallogr.* **1998**, *C53*, 1314. For 2,12-dioxo- and 2,12-dithioporphyrins which are formally bacteriochlorins, see: Arasasingham, R. D.; Balch, A. L.; Olmstead, M. M. *Heterocycles* **1988**, *27*, 2111. Pandey, R. K.; Isaac, M.; McDonald, I.; Medforth, C. J.; Senge, M. O.; Dougherty, T. J.; Smith, K. M. *J. Org. Chem.* **1997**, *62*, 1463. For methyl bacteriopheophorbide *a*: Barkigia, K. M.; Gottfried, D. S.; Boxer, S. G.; Fajer, J. *J. Am. Chem. Soc.* **1989**, *111*, 6444. Barkigia, K. M.; Gottfried, D. S. *Acta Crystallogr.* **1994**, *C50*, 2069.

(6) For a recent example of theoretical calculations based on protein data, see: Cory, M. G.; Zerner, M. C.; Hu, Z.; Schulten, K. *J. Phys. Chem. B* **1998**, *102*, 7640. For calculations based on higher precision, isolated bacteriochlorin structures, see: Facelli, J. C. *J. Phys. Chem. B* **1998**, *102*, 2111. Marchi, M.; Hutter, J.; Parrinello, M. *J. Am. Chem. Soc.* **1996**, *118*, 7847. Foloppe, N.; Breton, J.; Smith, J. C. *The Photosynthetic Reaction Center II*; Breton, J., Vermeglio, V., Eds.; Plenum Press: New York, 1992; p 43. Barkigia, K. M.; Miura, M.; Thompson, M. A.; Fajer, J. *Inorg. Chem.* **1991**, *30*, 2233. Gudowska-Nowak, E.; Newton, M. D.; Fajer, J. *J. Phys. Chem.* **1990**, *94*, 5795. Parson, W. W.; Creighton, S.; Warshel, A. *J. Am. Chem. Soc.* **1989**, *111*, 4277.

(7) For a recent review, see: Sternberg, E. D.; Dolphin, D.; Brückner, C. *Tetrahedron* **1998**, *54*, 4151.

(8) Zilberstein, J.; Bromberg, A.; Frantz, A.; Rosenbach-Belkin, V.; Kritzmann, A.; Pferfermann, R.; Solomon, Y.; Scherz, A. *Photochem. Photobiol.* **1997**, *65*, 1012.

(9) Schuitmaker, J. J.; deKoster, B. M.; Elferink, J. G. R. *Photochem. Photobiol.* **1998**, *68*, 841.

(10) Ressler, M. M.; Pandey, R. K. *Chemtech*, **1998**, 39.

(11) Morgan, A. R.; Gupta, S. *Tetrahedron Lett.* **1994**, *35*, 4291.

(12) Gunter, M. J.; Robinson, B. C. *Tetrahedron Lett.* **1990**, *31*, 285. Gunter, M. J.; Robinson, B. C. *Aust. J. Chem.* **1990**, *43*, 1839.

(13) Forsyth, T. P.; Nurco, D. J.; Pandey, R. K.; Smith, K. M. *Tetrahedron Lett.*, **1995**, *36*, 9093.

(14) Robinson, B. C. *Tetrahedron* 1999, Submitted for publication.

(15) Ridley, J.; Zerner, M. *Theor. Chim. Acta (Berlin)* **1973**, *32*, 111; **1976**, *42*, 223. Thompson, M. A.; Zerner, M. C.; Fajer, J. *J. Phys. Chem.* **1991**, *95*, 5693.

(16) Davis, M. S.; Forman, A.; Hanson, L. K.; Thornber, J. P.; Fajer, J. *J. Phys. Chem.* **1979**, *83*, 3325.

(17) Fajer, J.; Borg, D. C.; Forman, A.; Felton, R. H.; Dolphin, D.; Vegh, L. *Proc. Natl. Acad. Sci. U.S.A.* **1974**, *71*, 994. Chang, C. K.; Hanson, L. K.; Richardson, P. F.; Young, R.; Fajer, J. *Proc. Natl. Acad. Sci. U.S.A.* **1981**, *78*, 2652.

(18) Fajer, J.; Brune, D. C.; Davis, M. S.; Forman, A.; Spaulding, L. D. *Proc. Natl. Acad. Sci. U.S.A.* **1975**, *72*, 4956.

(19) Renner, M. W.; Zhang, Y.; Noy, D.; Scherz, A.; Smith, K. M.; Fajer, J. In *Reaction Centers of Photosynthetic Bacteria*; Michel-Beyerle, M. E., Ed.; Springer-Verlag: Berlin, **1996**; p 367.

(20) Hartwich, G.; Fiedor, L.; Simonin, I.; Cmiel, E.; Schäfer, W.; Noy, D.; Scherz, A.; Scheer, H. *J. Am. Chem. Soc.* **1998**, *120*, 3675.

(21) Barkigia, K. M.; Renner, M. W.; Furenlid, L. R.; Medforth, C. J.; Smith, K. M.; Fajer, J. *J. Am. Chem. Soc.* **1993**, *115*, 3627.

(22) Callahan, P. M.; Cotton, T. M. *J. Am. Chem. Soc.* **1987**, *109*, 7001. Cotton, T. M.; Van Duyne, R. P. *J. Am. Chem. Soc.* **1979**, *101*, 3981.

(23) Geskes, C.; Hartwich, G.; Scheer, H.; Mäntele, W.; Heintze, J. *J. Am. Chem. Soc.* **1995**, *117*, 7776.

(24) Fajer, J.; Davis, M. S. *The Porphyrins;* Dolphin, D.; Ed.; Academic Press: New York, 1979; Vol. IV, p 197.

(25) RHF/SP═Restricted Hartree−Fock/Spin Polarization. Plato, M.; Möbius, K.; Lubitz, W. *Chlorophylls*; Scheer, H., Ed.; CRC Press: Boca Raton, FL, 1991; p 1015.

(26) Plato, M.; Möbius, K.; Wittenberg, M. Private communication.

(27) Lubitz, W.; Lendzian, F.; Plato, M.; Scheer, H.; Möbius, K. *Appl. Magn. Reson.* **1997**, *13*, 531. Horning, T. L.; Fujita, E.; Fajer, J. *J. Am. Chem. Soc.* **1986**, *108*, 323. Borg, D. C.; Forman, A.; Fajer, J. *J. Am. Chem. Soc.* **1976**, *98*, 6689.